ISSN Print: 2394-7500
ISSN Online: 2394-5869
Impact Factor: 8.4
IJAR 2021; 7(1): 47-52
www.allresearchjournal.com
Received: 15-11-2020
Accepted: 23-12-2020

Dr. Manoj Kumar Sinha
Department of Physics,
Butwal Multiple Campus,
Tribhuvan University, Nepal

Corresponding Author:
Dr. Manoj Kumar Sinha
Department of Physics,
Butwal Multiple Campus,
Tribhuvan University, Nepal

Analysis of mathematical modelling of a solar parabolic collector

Dr. Manoj Kumar Sinha

Abstract
The main objective in this paper, a thermal model of a solar parabolic through collector is present. Numerical simulations of the model are performed in Matlab. Temperature evaluation at different nodes is presented and a comparison between a different solar collectors is made.

Keywords: Analysis, mathematical, modelling, parabolic, collector

Introduction
Recently, the environmental consequences have forced many nations in the world to harvest the abundant solar energy for their domestic and industrial applications. Solar thermal systems, in addition to the well-known advantages of renewable resources are very suitable for air-conditioning and refrigeration demands, because solar radiation availability and cooling requirements usually coincide [1, 2].

Solar air-conditioning and refrigeration facilities can also be easily combined with space heating and hot water applications, increasing the yearly solar fraction of buildings. Conventional cold producing machines that are based on vapor compression principle are primary electricity consumers and their working fluids are being banned by international legislation. Solar powered cooling systems as a green cold production technology are the best alternative. Absorption refrigeration is a mature technology that has proved its applicability with the possibility to be driven by low grade solar and waste heat [3].

Xu *et al*. [4] presented a study on the comparison of three outdoor test methods for determining the thermal performance of parabolic trough solar collectors. The methods are respectively the steady-state method in the ASHRAE 93 standard, the quasi-dynamic method in the EN 12975-2 standard and a new dynamic method developed by the authors. The comparison shows the advantages and disadvantages of these models according to both the practical operation and weather conditions.

A detailed numerical heat transfer model based on the finite volume method is presented by Hachicha *et al*. [5] the different elements of the receiver are discretized into several segments in both axial and azimuthal directions. The set of algebraic equations are solved simultaneously using direct solvers. Results obtained shown a good agreement with experimental data. As shown in Figure 1,

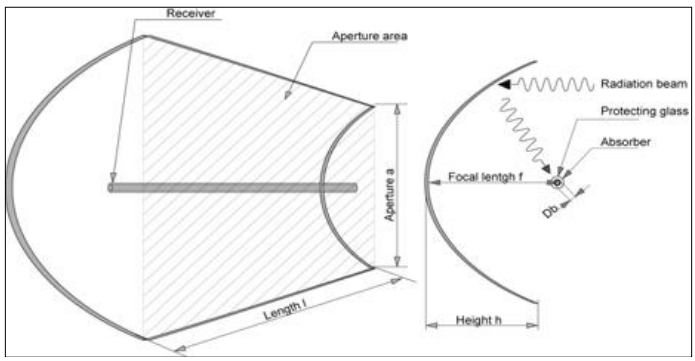

Fig 1: Geometry of the solar parabolic trough collector

Formulation

The linear parabolic concentrator form is given by:

$y^2=4fx$ (1)

where f is the focal length of the collector.

Thermal energy received at the focal line is absorbed by a metallic pipe inside an evacuated glass tube. The geometric concentration ratio is a measure of the average concentration. Its value depends directly on the collector geometry. It can be calculated by the ratio of the collector aperture area (A_a) to the receiver area (A_r) [6]:

$$C = \frac{A_a}{A_r} \quad (2)$$

The actual concentration coefficient is calculated using the following equation [7]:

$$A_a = l\left[\left(\frac{a}{2}\sqrt{\left(\frac{4h}{a}\right)^2+1}\right)+2f\ln\left(\frac{4h}{a}\sqrt{\left(\frac{4h}{a}\right)^2}\right)\right] \quad (3)$$

With

$$h = \frac{a^2}{16f} \quad (4)$$

$$A_r = \pi l D_h$$

a and l are respectively the collector aperture diameter and the length of the concentrator, Db is the mean diameter of the absorber.

In dynamic modeling, energy stored in certain levels is considered. These levels are considered as nodes at a uniform temperature. This method consists in subdividing a system into several subsystems. But before establishing the energy balance of the collector, modeling assumptions must be considered. The following simplifying assumptions have been made:

- Due to vacuum, heat transfer between the glass and the absorber is only due to radiation and conduction and therefore convection is negligible [8].
- The working fluid is incompressible and without phase change.
- The absorbent tube coincides with the focal line.
- The temperature is uniform at each node.
- The glass is considered opaque to infrared radiation.
- Temporal variations along the absorber and the glass thickness are negligible.
- The solar flux at the absorber is uniformly distributed.

Mathematical modeling

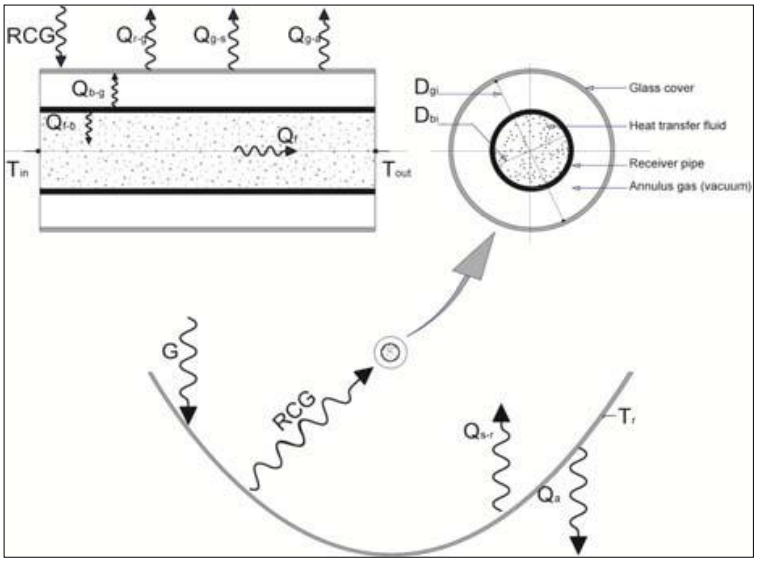

Fig 2: Energy balance

Figure 2 shows the different types of heat transfer involved. According to this representation, a homogeneous temperature prevails at each node and an axisymmetric heat transfer occurs. An electrical analogy of the problem is shown in Figure 3.

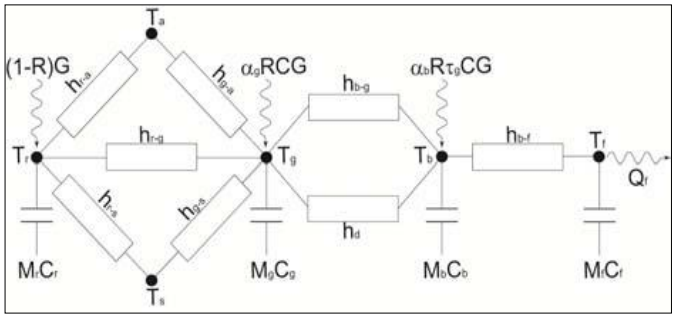

Fig 3: Electrical analogy of the problem

The amount of heat exchanged between the nodes can be written as:

$$Q_{ij} = A_{ij}h_{ij}(T_i - T_j) \quad (5)$$

i and j are the two neighboring nodes, A_{ij} and h_{ij} are respectively the surface and heat transfer coefficient between the two i and j nodes.

Each node stores a quantity of heat which depends on the capacity of the used material. Temperature change over time is given by:

$$Q_i = M_i C_i \frac{dT_i}{dt} \quad (6)$$

Heat transfers between reflector and air is given by:

$$M_r C_r \frac{dT_r}{dt} = \begin{pmatrix} (1-R)G - h_{r-a}(T_r - T_a) \\ -h_{s-r}(T_r - T_s) - h_{r-g}(T_r - T_g) \end{pmatrix} \quad (7)$$

Between glass and reflector, it's expressed by

$$M_g C_g \frac{dT_g}{dt} = \alpha_g A_g RG + A_g h_{r-g}(T_r - T_g) - A_{ge}\left(h_{g-a}(T_g - T_a) + h_{s-g}(T_g - T_s)\right) + A_{gi}\left(h_{b-g} + h_d\right)(T_b - T_g) \quad (8)$$

Similarly by absorber and glass

$$M_b C_b \frac{dT_b}{dt} = \tau_g \alpha_b A_r RG - A_{bi} h_{b-f}(T_b - T_f) - A_{gi}\left(h_{b-g} + h_d\right)(T_b - T_g) \quad (9)$$

And finally between HTF and absorber

$$M_f C_f \frac{dT_f}{dt} = A_{pi} h_{p-f}(T_p - T_f) - \dot{m} C_f \frac{dT_f}{dx} \quad (10)$$

With M_i and C_i is the mass and specific heat of the i node material, m_f is the working fluid mass flow, T_s the sky temperature calculated by [9]:

$$T_s = 0.0552 T_a^{1.5} \quad (11)$$

Many empirical correlations are used to determine directly the heat transfer coefficients between the different nodes.
Reflector and sky [8].

$$h_{s-r} = \sigma \varepsilon_r (T_s + T_r)(T_s^2 + T_r^2) \quad (12)$$

Reflector and glass [15, 16].

$$h_{r-g} = \frac{\sigma\left(T_g^2 + T_r^2\right)\left(T_g + T_r\right)}{\frac{1-\varepsilon_g}{\varepsilon_g} + \frac{1}{F_{rg}} + \frac{(1+\varepsilon_r)A_r}{\varepsilon_r A_{ge}}} \quad (13)$$

With

$$F_{rg} = \frac{\left[\left(W_1 + W_2\right)^2 + 4\right]^{\frac{1}{2}} - \left[\left(W_2 - W_1\right)^2 + 4\right]^{\frac{1}{2}}}{2W_1}$$

$$W_1 = \frac{D_{ge}}{f}$$

$$W_2 = \frac{a}{f}$$

Between reflector and air [10].

$$h_{r-a} = \frac{8.6 V^{0.6}}{l^{0.4}} \quad (14)$$

Between glass and sky [8].

$$h_{s-g} = \sigma \varepsilon_g (T_s + T_g)(T_s^2 + T_g^2) \quad (15)$$

Between glass and air [4].

$$h_{g-a} = \frac{4V^{0.58}}{D^{0.42}}$$

Between glass and absorber [6, 8, 11, 12].

$$h_{b-g} = \frac{\sigma\left(T_g^2 + T_b^2\right)\left(T_g + T_b\right)}{\frac{1-\varepsilon_g}{\varepsilon_g} + \frac{1}{F_{gb}} + \frac{(1+\varepsilon_b)A_{gi}}{\varepsilon_b A_{be}}} \quad (16)$$

With

$$F_{gb} = \frac{1}{X}\left[\frac{1}{\pi}\left(\cos^{-1}\left(\frac{B}{A}\right)\frac{1}{2Y}\left(C\cos^{-1}\left(\frac{B}{XA}\right) + B\cos^{-1}\left(\frac{1}{X}\right) - \frac{\pi}{2}A\right)\right)\right]$$

$$X = \frac{D_{gi}}{D_{be}}, \quad Y = \frac{2l}{D_{be}},$$

$$A = X^2 + Y^2 - 1, \quad B = X^2 Y^2 - 1, \quad C = \sqrt{(A+2)^2 - (2X)^2}$$

Between absorber and fluid [13].
For turbulent flow, $Re > 10^4$:

$$Nu\ 0.125\ (0.790 \log (Re)\ 1.64)^{-2}\ RePr^{0.34} \quad (18)$$

For laminar flow, $Re < 10^4$

$$Nu = 3.66 + \frac{0.0668\left(\frac{D_{bi}}{l}\right)\mathrm{Re}\,\mathrm{Pr}}{1 + 0.04\left[\left(\frac{D_{bi}}{l}\right)\mathrm{Re}\,\mathrm{Pr}\right]^{0.67}} \quad (19)$$

Solar parabolic trough collector behavior

Programming equations of the parabolic is performed in Matlab. Iterative Gauss method is used to solve these equations after finite difference discretization. The Parabolic trough solar collector unsteady equations are discretized and solved by the finite volume method. A Crank-Nicolson scheme with t=1s was adopted for the time step.

Calculations are performed using a uniform mesh containing 100 nodes, iterative Gauss method was used and the program was written in Matlab. The collector components' geometrical and thermo physical properties and HTF properties are summarized in Table 1 and Table 2.

Table 1. And 2 illustrate respectively the collector components geometrical and thermal properties and HTF properties.

Table 1: Collector properties

	Symbol	Parameter	Value	Unit
Collector	l	Collector length	7.800	m
	a	Aperture	5.000	m
	f	Focal length	1.840	m
Reflector	Cp_r	Specific heat	0.581	$kJ/(kg.K)$
	ρ_r	Density	2,400	kg/m^3
	e_r	Thickness	0.005	m
	ε_r	Emittance	0.140	–
	R_r	Reflectance	0.930	–
Glass	Cp_g	Specific heat	1.090	$kJ/(kg.K)$
	ρ_g	Density	2,230	kg/m^3
	D_{gi}	Internal diameter	0.107	m
	D_{ge}	External diameter	0.114	m
	τ_g	Transmittance	0.935	–
	ε_g	Emittance	0.860	–
	α_g	Absorptance	0.020	–
Absorber	Cp_b	Specific heat	0.500	$kJ/(kg.K)$
	ρ_b	Density	8,020	kg/m^3
	D_{bi}	Internal diameter	0.066	m
	D_{be}	External diameter	0.0 0	m
	ε_b	Emissivity	0.140	–
	α_b	Absorptance	0.905	–
	p_v	Vacuum pressure	0.010	bar

Table 2: Fluid Properties

Parameter	Value	Unit
Specific heat	1,616	$kJ/(kg.K)$
Density	935	kg/m^3
Conductivity	0.134	$W/(m.K)$
Viscosity	9.1	$Pa.s$
Critical temperature	367	$°C$
Critical pressure	10.7	bar
Critical density	3.22	l/kg

Result and Discussion

According to Figure 4 shows a comparison of the evolution the outlet HTF temperature with respect to the temperature above ambient between model predictions and test data of the LS-2/Schott HCE. Except the first value, a good agreement is found that the difference between predicted and experimental values of temperature does not exceed one degree (1K).

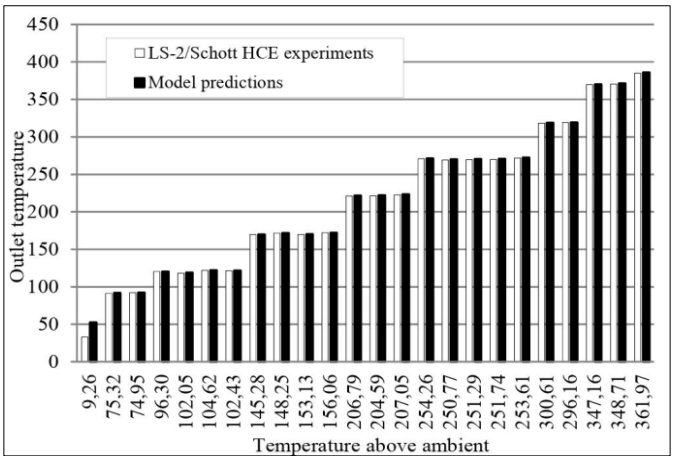

Fig 4: Outlet HTF temperature vs. temperature above ambient

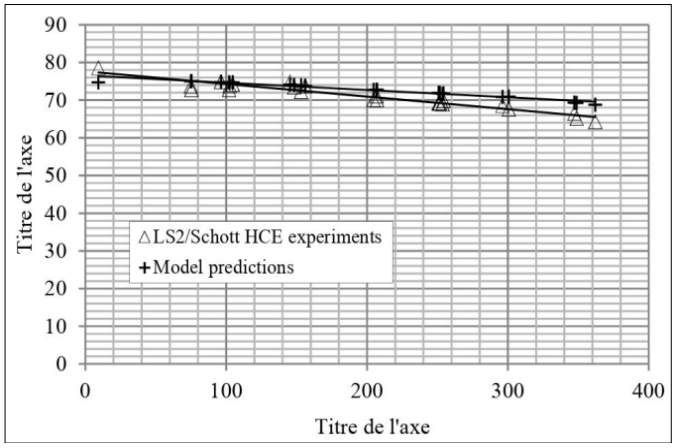

Fig 5: Peak efficiencies vs. average HTF temperature through the HCE above ambient

Similarly, figure 5 shows a comparison between predicted and measured peak efficiencies versus the HTF temperature above ambient. Here again, a good agreement is found. Nevertheless, a maximum prediction error of 6.56% is observed between predicted and measured values changes according to the temperature to obtain

These results allow for the use of the model for predicting the approximate temperature of the fluid outlet and the energy required to activate desorption of the binary solution in the absorption machine.

Simulations allow studying the temperature evolution and hence the effectiveness of the collector at any time of the day throughout the year. Temperature evolution at each node is in a good agreement with the studied literature. Absorber temperature is greater compared to other temperatures due to its position in the focal line and its absorptivity, as shown in Figure 6.

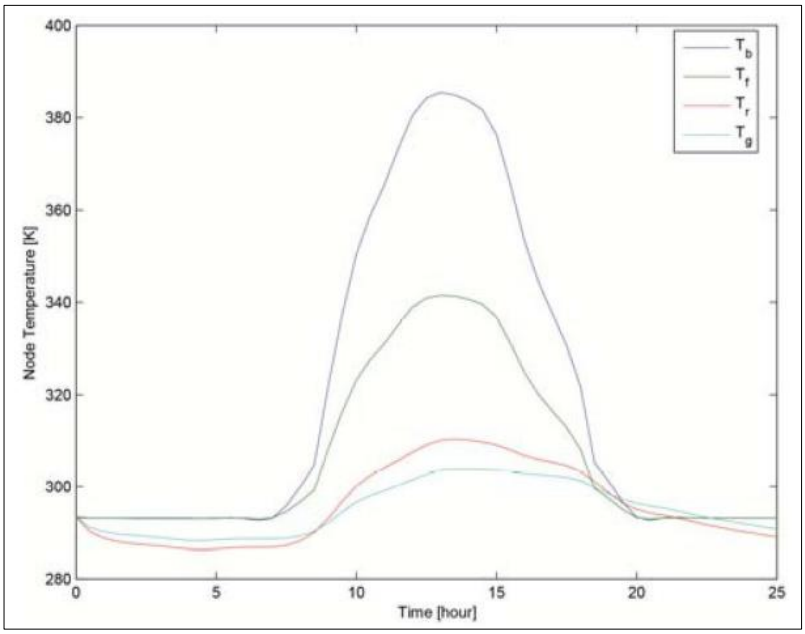

Fig 6: Daily Temperature evolution at the different nodes

Simulations allow also studying the efficiency of some collectors and to detect the most suitable energy solution. As shown in Figure 7

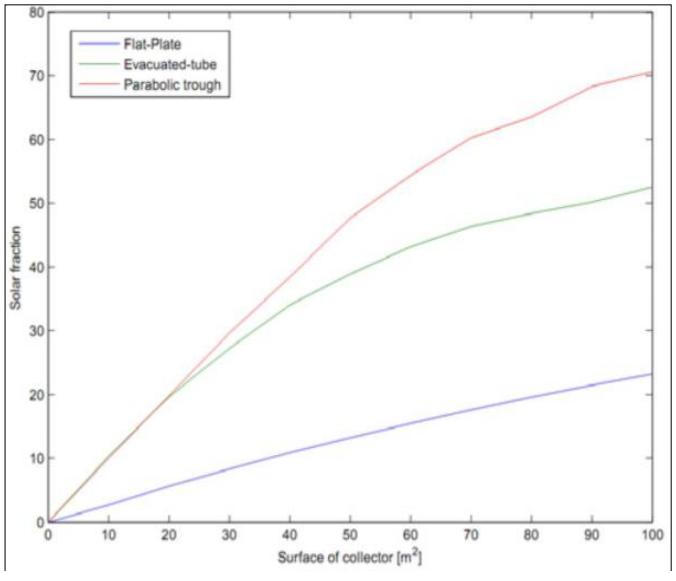

Fig 7: Solar fraction for different collector types

Illustrates a comparison of collectors' solar fractions relative to the surface and allows choosing the most appropriate collector for the solar cooling installation, thus optimizing its surface. It shows that the flat plate collector has the lowest solar fraction compared to the two other collectors. For the two others, the preference depends on climatic conditions and surface. For small areas, the evacuated tube collector is more convenient. But when using larger areas, the concentration collector becomes the most reliable.

Conclusion

The present paper phasing between the need for cold and Solar gain in generally excellent, with sometimes a slight delay which can be compensated by storage. The use of solar energy for air–conditioning is a promising alternative.

References

1. Kalkan N, Young EA, Celiktas A. Solar thermal air conditioning technology reducing the footprint of solar thermal air conditioning Renewable and Sustainable Energy Reviews 2012;16:6352–83.
2. Kim DS, Infante Ferreira CA. Solar refrigeration options-a state-of the-art review", International Journal of Refrigeration 2018;31:3–15

3. Igor G Dyominov, Alexander M Zadorozhny. Greenhouse gases and recovery of the Earth's ozone layer, advances in space research 2015.
4. Li Xu, Zhifeng Wang, Xin Li, Guofeng Yuan, Feihu Sun, Dongqiang Lei, *et al*. A comparison of three test methods for determining the thermal performance of parabolic trough solar collectors, Solar Energy 2014;99:11–2.
5. Hachicha AA, Rodríguez I, Capdevila R, Oliva A. Heat transfer analysis and numerical simulation of a parabolic trough,solar collector", Applied Energy 2013;111:581-592.
6. Duffie JA, Beckman WA. Solar Engineering of Thermal Processes, 3rd Edition, John Wiley & Sons, USA 2006.
7. Kim DS, Infante Ferreira CA. Solar refrigeration options-a state-of the-art review, International Journal of Refrigeration 2008;31:3–15.
8. Modest MF. Radiative Heat Transfer, Elsevier Science, USA 2003.
9. Price H, Lüpfert E, Kearney D, Zarza E, Cohen G, Advances in parabolic trough solar power technology, Journal of Solar Energy Engineering 2002;124(2):109-25.
10. Kalogirou S. Solar Energy Engineering, Elsevier Inc, USA, 2009.
11. Naeeni N, Yaghoubi M. Analysis of wind flow around a parabolic collector (2) heat transfer from receiver tube 2017;32(8):1259-1272.
12. Ratzel AC, Hickox CE, Gartling DK. Techniques for reducing thermal conduction and natural convection heat losses in annular receiver geometries, J Heat Transfer, 2019, 108-113.
13. Holman JP. Heat transfer, McGraw-Hill, Singapora, 2020.